Magazine of Civil Engineering

ISSN 2712-8172

journal homepage: http://engstroy.spbstu.ru/

Research article

UDC 624.012.45:539.376

DOI: 10.34910/MCE.139.2

Stress relaxation behavior of glass and carbon fiber reinforcements in prestressed concrete applications

P.S. Mostovykh , ***A.E. Dontsova*** , ***T.A. Koriakovtseva*** , ***O.N. Stolyarov***

Peter the Great St. Petersburg Polytechnic University, St. Peterburg, Russian Federation

✉ *anne.dontsoova@gmail.com*

Keywords: prestressed concrete, stress relaxation, fiber reinforcement, roving, viscoelasticity, modeling

Abstract. High-performance fibrous materials offer advantages such as high strength and low weight, making them promising for use in prestressed concrete. This work investigates the stress relaxation behavior of glass and carbon fiber reinforcements. Stress relaxation tests were conducted at load levels ranging from 10 % to 40 % of the materials' tensile strength. A mathematical model was developed to describe this behavior, and the model parameters were determined. The stress relaxation of the fiber reinforcements was simulated and the resulting prestress loss was compared with that of traditional steel reinforcement. It was found that stress relaxation is more pronounced in glass and carbon fiber reinforcements than in steel. It was shown that the observed stress loss is primarily caused by the slippage of the fibrous reinforcement. Based on the findings, practical recommendations are provided for the application of these results in prestressed concrete design.

Funding: The research was funded by the Russian Science Foundation (project No. № 25-29-00771).

Citation: Mostovykh, P.S., Dontsova, A.E., Koriakovtseva, T.A., Stolyarov, O.N. Stress relaxation behavior of glass and carbon fiber reinforcements in prestressed concrete applications. Magazine of Civil Engineering. 2025. 18(7). Article no. 13902. DOI: 10.34910/MCE.139.2

1. Introduction

Prestressed concrete structures traditionally offer several advantages compared to conventional reinforced concrete structures [1]. The main advantage is the reduction in the structure's mass and size due to the more efficient use of reinforcement. Prestressed structures with steel reinforcement have been used in the manufacture of concrete products for several decades. Alongside metal reinforcement, composite reinforcement is now being used for reinforcing concrete [2–8]. Various yarns, rovings, straps, sheets, and plates made of high-performance fibers such as glass, basalt, and carbon are used as reinforcement [9]. Its mechanical characteristics are on par with those of steel reinforcement, and due to its corrosion resistance and resilience to aggressive environments, it may even surpass steel reinforcement.

The properties of the fibrous reinforcement vary and depend heavily on the properties of the original fiber. The most common types involve the use of glass (glass fiber reinforced polymer, GFRP) or carbon (carbon fiber reinforced polymer, CFRP) fibers. In the latter case, Young's modulus is comparable to that of the steel reinforcement. Furthermore, if we consider that there is no need to create a concrete protective layer of several centimeters thick, then concrete structures with such reinforcement possess an undeniable advantage. Such structures have found wide application in the building envelopes and other areas over the last two decades. Similar to prestressed steel reinforced concrete, numerous attempts have recently been made to use pre-tensioning in composite concrete structures. The principle of reinforcement is the same as that of steel reinforcement: a carbon mesh is pre-tensioned to a specified stress value, and then the concrete is cast [10, 11]. In [12, 13], the influence of the number of layers and the level of pre-tensioning

on the bending characteristics of textile concrete reinforced with basalt and carbon rovings was investigated. In addition to the undeniable advantages of using composite reinforcement, which include the absence of corrosion, there are several disadvantages inherent primarily to fibrous reinforcement. One of the obvious difficulties in the successful application of composite reinforcement in prestressed structures is the process of loss of internal stress over time, i.e., the instability of the reinforcing mesh properties. A drop in stress in the composite reinforcement can negate all the advantages of a pre-stressed concrete structure [14–19]. Li et al. [14] studied the transverse compression stress relaxation behavior under different stress levels. The relaxation characteristics were analyzed, and the stress-relaxation model was proposed. Under the stress level from 30% to 80%, the long-term stress relaxation ratio was between 19 % and 33 %. Wang et al. [15] showed that the prestress losses of CFRP are due to the anchorage set and the time-dependent behavior. The stress losses are approximately from 12.6 % to 18.2 % and from 2.3 % to 3.9 % of the initial prestress for anchorage and stress relaxation, respectively. Therefore, it is relevant to study the processes of internal stress loss, the so-called stress relaxation, in composite reinforcement.

A drop in stress over time also occurs in traditional steel reinforcement. Therefore, the design of the prestressed reinforcement also accounts for the possible stress loss. This accounting involves adopting various coefficients that consider the effects related to stress relaxation in the reinforcement itself, losses during concrete heating, losses due to concrete shrinkage, and concrete creep. These processes are well studied, and regulatory documents provide various coefficients and formulas that allow for estimating the level of pre-tension loss in steel reinforcement [20].

Unlike steel reinforcement, the nature of these processes in fibrous reinforcement is somewhat different, although some similar aspects can be found. For example, stress relaxation can occur in the reinforcement itself, and there can also be slippage due to the method for anchoring [21–23]. Furthermore, since composite reinforcement consists of high-strength rovings, each composed of several thousand individual filaments that are in contact with each other and with the concrete matrix, interfibrillar friction occurs within the core of the reinforcing component [24]. Also, with an increase in the prestress level, the stress drop in the fibrous reinforcement increases. This is associated with a significant reduction in the cross-sectional dimensions under tension: the fibers group together in the center, migrating from the outside inward, the cross-section reduces sharply, which also affects the stress loss. Similar problems related to stress loss due to anchorage are observed; this process is accompanied by much greater losses because it is very difficult to anchor brittle, high-strength rovings. As mentioned above, carbon rovings are primarily used, which have minimal elongation at break (1–2 %) and are extremely brittle. Therefore, the traditional tensioning methods cannot be applied to these reinforcing meshes. Various materials, such as epoxy resin, must be used to prevent mechanical damage to the ends of the reinforcing mesh. In practice, pre-prepared molds are used to anchor the carbon composite reinforcement, and the ends of the rovings are potted in epoxy resin. After hardening, this allows the reinforcement to be placed in a clamping device and securely fixed.

A literature review revealed a lack of studies specifically focused on investigating stress relaxation processes in prestressed concrete reinforcement. However, there is research related to the study of the creep behavior of high-strength fiber reinforced concrete, which, in principle, provides analogous information and can be considered when developing predictive models for stress relaxation. In [25], the influence of fibers on the creep behavior of fiber-reinforced concrete was studied. It was shown that the creep strain is significantly influenced by the Young's modulus of the fiber and the matrix as well as the fiber length and thickness. The time-dependent behavior of the textile-reinforced concrete was studied via flexural creep [26]. A viscoelastic model was successfully developed to predict the creep deformation of the concrete composite. It can be stated that the processes of stress relaxation in composite reinforcement have been poorly studied. There is only data from testing similar composite materials, but studies specifically concerning pre-stressed composite reinforcement in concrete are practically absent, and no publications by authors on this topic were found. This underscores the relevance of this work. The aim of this work is to study the stress relaxation behavior of glass and carbon fiber reinforcements under different prestress levels and to understand the prestress losses in the fibrous reinforcement applied to the prestressed concrete composites.

The objectives of this work are:

- to conduct experimental studies of the stress relaxation in continuous glass and carbon rovings under different load levels;
- to propose a mathematical model for stress relaxation that accounts for the fiber properties and the initial prestress level;
- to develop a technical approach for measuring stress relaxation in composite reinforcement, comparable to the methods used for traditional steel reinforcement.

2. Materials and Methods

2.1. Test Samples

This study focuses on two fibrous reinforcements made of glass and carbon rovings. Table 1 lists the characteristics of the samples. The ends of the brittle glass and carbon rovings were clamped in a mold, and epoxy resin was poured into the mold to prevent damage to the rovings. Fig. 1a illustrates the setup for testing the roving sample.

Table 1. Characteristics of materials tested.

Sample designation	Raw material	Linear density (tex)	Cross-sectional area (mm^2)	Tensile strength (MPa)	Young's modulus (GPa)
AG	AR-Glass roving	2400	0.896	708	66
CR	Carbon roving, PAN-based, 24K	1600	0.879	2015	173

2.2. Stress Relaxation Testing

Stress relaxation tests were conducted using an Instron universal tensile testing machine (model 5965). The stress relaxation behavior of the glass and carbon rovings was evaluated at various loading levels. The test programs for the stress relaxation and inverse stress relaxation loadings are shown in Table 2. The stress relaxation loadings are shown schematically in Fig. 2b.

The tensile stress of the fabrics (MPa) was calculated by the following formula:

$$\sigma = \frac{F\gamma}{T}, \tag{1}$$

where F is the maximal applied force (N), γ is roving density (kg/m^3), and T is the nominal linear density of the roving (tex).

Table 2. A list of test programs.

No	σ_{rel} (MPa)	as % of σ_{max}	t_{rel} (s)	σ_{3600} (MPa)	σ_{ir} (MPa)	t_{ir} (s)	σ_{7200} (MPa)
Glass roving							
AG-1	70.8	10	3600	62.1	52.1/50.4	3600	50.3
AG-2	140.5	20	3600	124.0	52.1/50.9	3600	52.4
AG-3	211.2	30	3600	183.1	41.6/40.8	3600	57.3
AG-4	280.5	40	3600	247.5	52.1/51.1	3600	59.7
Carbon roving							
CR-1	201.5	10	3600	–	47.3	3600	55.6
CR-2	401.0	20	3600	–	49.3	3600	70.0
CR-3	601.8	30	3600	–	47.3	3600	76.0
CR-4	801.9	40	3600	–	48.1	3600	83.2

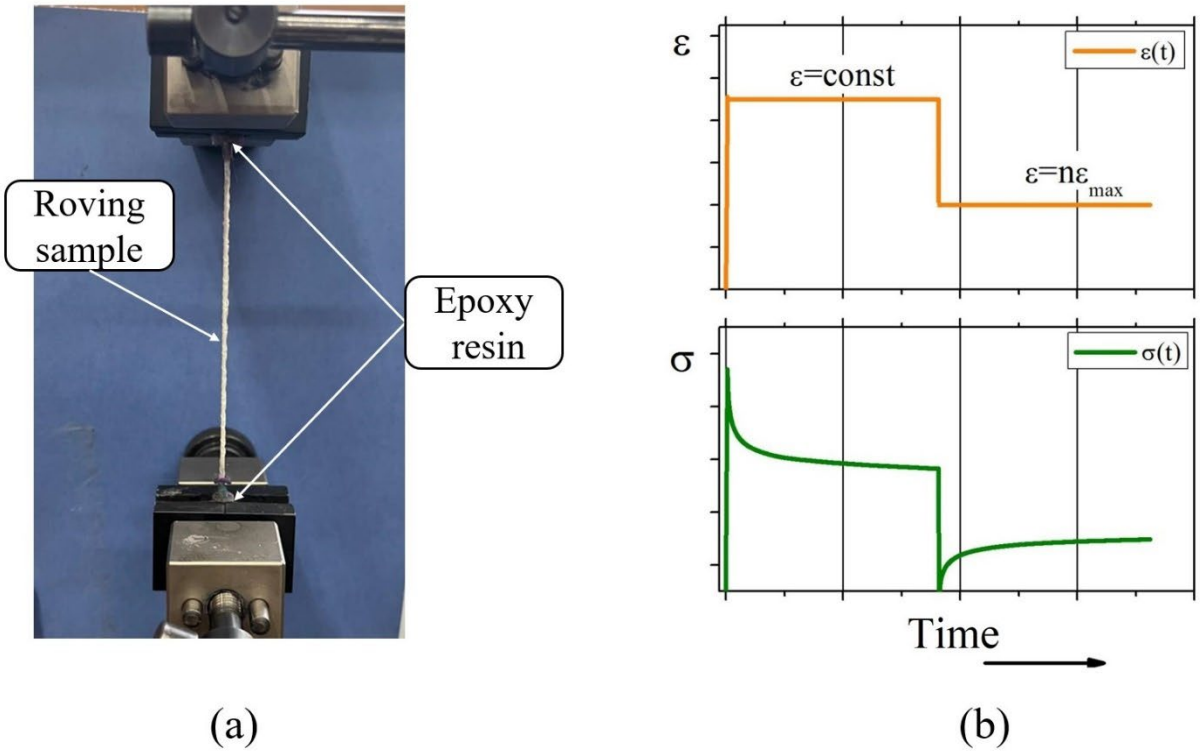

Figure 1. Experimental setup for testing the roving sample (a) and stress relaxation stages examined in this study (b).

3. Results and Discussion

3.1. Stress Relaxation and Inverse Stress Relaxation Tests

Stress relaxation and inverse stress relaxation tests were performed for the glass and carbon roving samples for fixed strain levels that varied from 10 % to 40 % of the tensile strength of the corresponding reinforcing material. Fig. 2 shows the experimentally obtained stress relaxation and inverse stress relaxation for each of the two rovings. Fig. 2a describes the stress relaxation behavior in time for the glass roving, and Fig. 2b describes the stress relaxation behavior in time for the carbon roving.

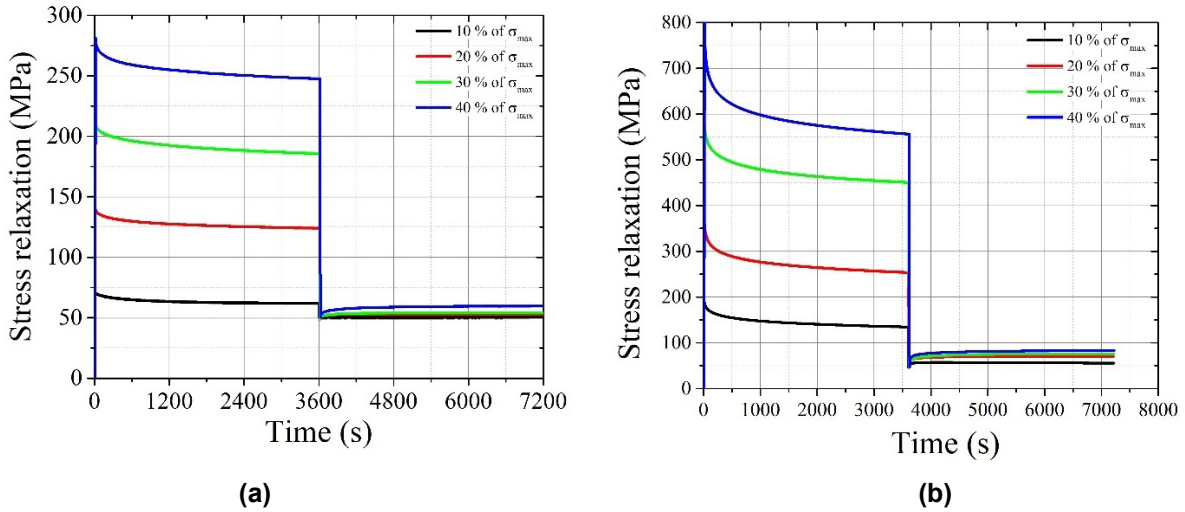

Figure 2. Experimental stress relaxation and inverse stress relaxation curves: glass roving (a), carbon roving (b).

The relaxation modulus curves obtained for the glass and carbon roving samples at various values of tensile stress and strain up to 40 % of the tensile strength were obtained according to the following formula:

$$E_{rel}(t_{rel}) = \frac{\sigma_{rel}}{\varepsilon_0} \quad [MPa], \tag{2}$$

where the relaxation time t_{rel} is calculated from the moment of the beginning of the stress relaxation test (from the moment when the deformation ε_0 is kept constant). In this work, the relative stress is used at relaxation, given by the expression:

$$\xi = \frac{\sigma_{rel}(t_{rel})}{\sigma_{rel}(0)} \quad [MPa/MPa], \tag{3}$$

i.e., the ratio of the stress in the relaxation test to the initially applied stress. Similarly, for inverse stress relaxation, the relative stress during inverse stress relaxation is determined by the following formula:

$$\chi = \frac{\sigma_{ir}(t_{ir}) - \sigma_{ir}(0)}{\sigma_{ir}(0) - \sigma_{rel}(3600)} \quad [MPa/MPa], \tag{4}$$

where the time of reverse relaxation t_{ir} is calculated from the moment of the beginning of the process of inverse stress relaxation, and $\sigma_{rel}(3600)$ represents the stress at the end of the relaxation process and is given in Table 1.

The stress relaxation curves plotted for the dimensionless parameter according to (3) are presented in Fig. 3, and the inverse stress relaxation curves plotted for the dimensionless parameter according to (4) are presented in Fig. 4.

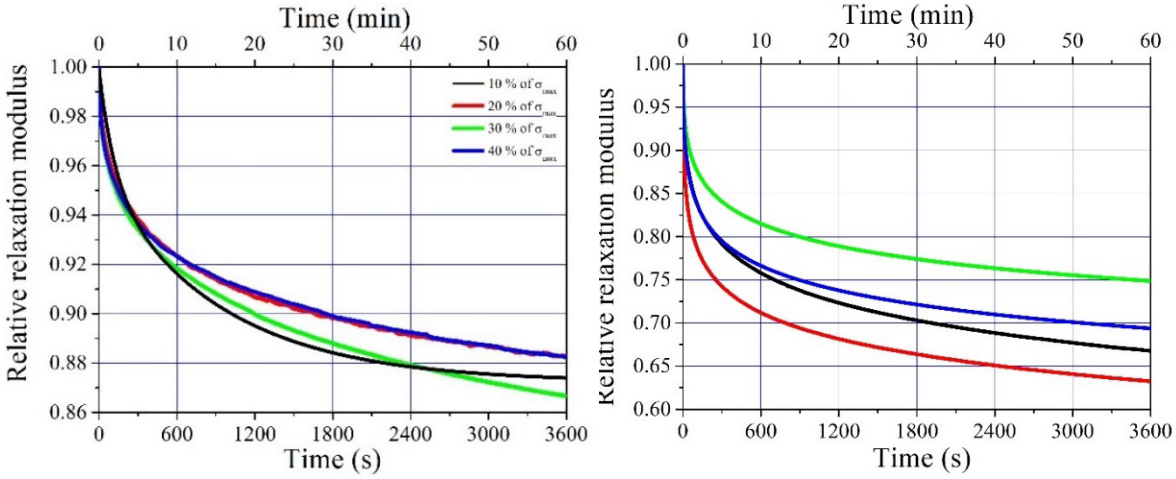

Figure 3. Stress relaxation: glass roving (a), carbon roving (b).

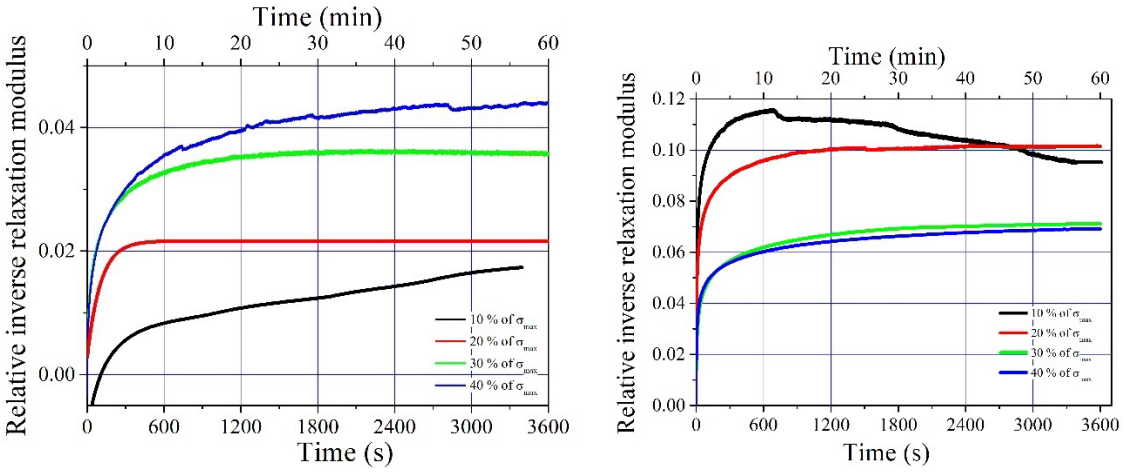

Figure 4. Inverse stress relaxation curves: glass roving (a), carbon roving (b).

As shown in Fig. 3, the stress relaxation curves for the glass roving practically coincide with each other, and the difference in the curves for the carbon roving is not related to the stress, at which the stress relaxation test was carried out. This indicates significant inconsistency of the carbon roving properties when changing from one sample to another. To develop a mathematical model, the average value of the relative relaxation modulus for each value of time was averaged. The best fitting for both the glass and carbon roving was given by the Belehradek formula:

$$1-\frac{\sigma_{rel}(t_{rel})}{\sigma_{rel}(0)}=a\left(\lg t_{rel}\text{-}b\right)^{c}, \tag{5}$$

where the logarithm is calculated from the time measured in seconds, and the values of parameters a, b, c for the tested materials are shown in Table 3.

According to the Belehradek formula, the amount of loss of the applied voltage was calculated for 1 hour, 1 day, 1 week and 1 month (30 days). The corresponding results are also presented in Table 3.

Table 3. Stress relaxation parameters in the glass and carbon rovings as described by the Belehradek formula.

Sample	Belehradek's parameters			Stress decay $\Delta\sigma/\sigma(0)$			
	a	*b*	*c*	1 hour	1 day	1 week	1 month
AG	0.00297	–0.99568	2.472181	12.8	24.2	33.7	42.0
CR	0.02972	–0.99568	1.55988	31.6	47.8	58.8	67.6

3.2. Characterization of Stress Relaxation Behavior

The best fit for the glass fiber was given by the Belehradek formula (5):

$$\sigma_{rel}(t_{rel})=\sigma_{rel}(0)\left(1-0.00297\left(\lg t_{rel}+0.99568\right)^{2.472181}\right),$$

and for the carbon fiber, in addition to the Belehradek formula:

$$\sigma_{rel}(t_{rel})=\sigma_{rel}(0)\left(1-0.00297\left(\lg t_{rel}+0.99568\right)^{1.55988}\right).$$

A good fit was also obtained using a third-degree polynomial fit to the logarithm of time.

$$\sigma_{rel}(t_{rel})=\sigma_{rel}(0)\left(0.97844-0.00397\lg t_{rel}-0.01955\lg^{2} t_{rel}+0.00213\lg^{3} t_{rel}\right).$$

A comparison of the predictions of these three formulas with the experimental data in semilogarithmic coordinates is shown in Fig. 5.

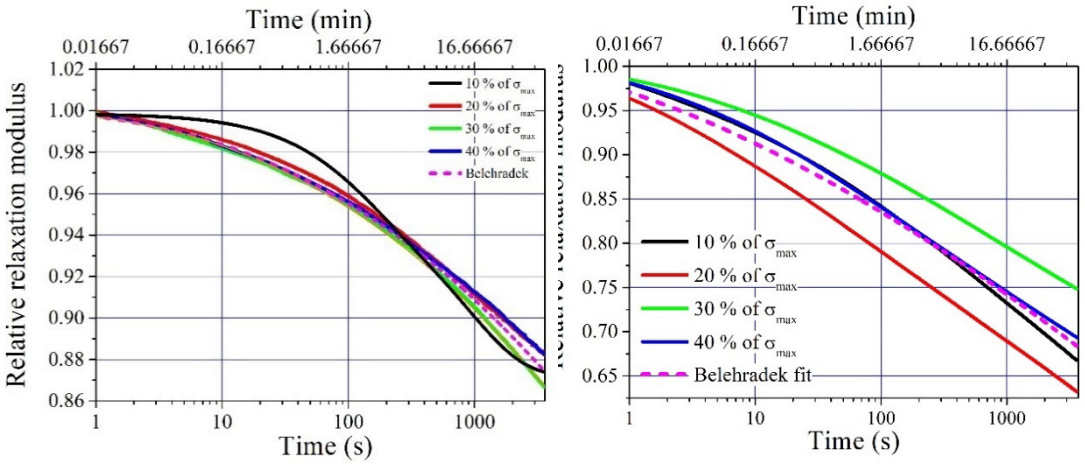

(a) **(b)**

Figure 5. Stress relaxation curves for the glass (a) and carbon (b) rovings and their approximation using Belehradek's formula and a third-degree polynomial in the logarithm of time (for the carbon roving only).

Based on the stress relaxation data, it can be assumed that the material is linearly viscoelastic. This assumption can be tested using the inverse stress relaxation data. Inverse stress relaxation is generally the sum of two processes: the elastic after effect from the unloading process (this part involves the increase in stress over time) and the elastic after effect from the loading process (this part involves the decrease in stress over time). The first of these parts, if the material is linearly viscoelastic, can be determined from the direct stress relaxation data; to estimate the second part, we extrapolate the stress relaxation curve in semi-logarithmic coordinates. Mathematically, then, the stress during inverse relaxation for glass roving will be expressed by the following formula:

$$\sigma_{ir}(t_{ir}) = \sigma_{rel}(0)\left(1 - 0.00297\left(\lg\left(t_{ir} + 3600\right) + 0.99568\right)^{2.472181}\right) -$$

$$-\left[\sigma_{ir}(0) - \sigma_{rel}(3600)\right]\left(1 - 0.00297\left(\lg t_{ir} + 0.99568\right)^{2.472181}\right),$$

and a similar expression can also be written for carbon roving. However, a comparison of the predictions of this formula (which expresses the hypothesis of linearity of the viscoelastic properties of glass and carbon fiber) and actual experimental data shows that the phenomenon of inverse stress relaxation for glass fiber is approximately 2.5 times smaller in magnitude than that predicted by linear theory and more than 3 times smaller for carbon rovings (Fig. 6). In other words, in the studied materials, the relaxation of nonequilibrium processes aimed at increasing the length of the sample occurs faster than the inverse process aimed at decreasing the sample's length.

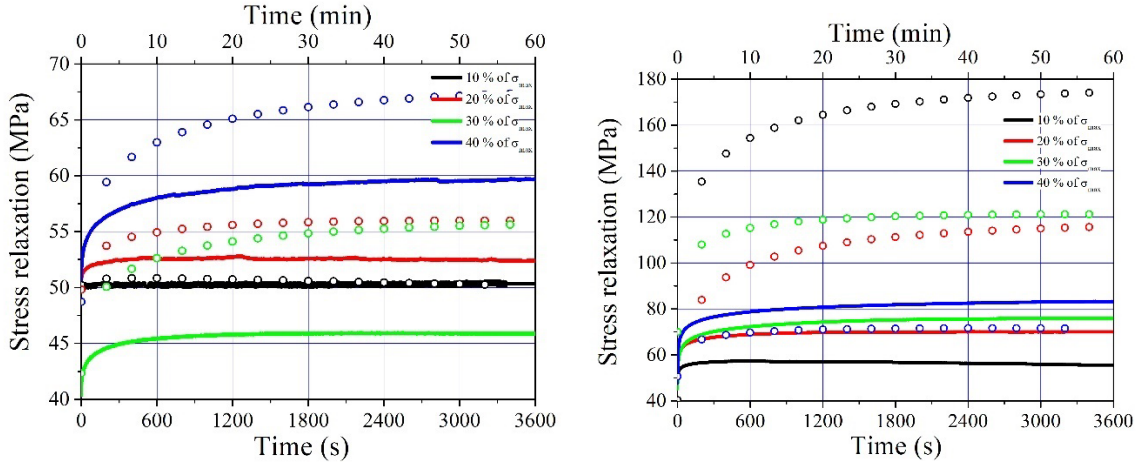

Figure 6. Inverse stress relaxation curves for glass fiber (a) and carbon fiber (b) and their theoretical prediction within the framework of linear viscoelasticity (Belehradek).

3.3. Comparison of the Obtained Data with the Stress Relaxation of Steel Reinforcement

According to [14], there are two types of stress relaxation losses. The first type is due to stress relaxation in the reinforcement, temperature changes during heat treatment of the structure, anchor deformation, and shape distortion. The second type is due to the shrinkage and the creep of the concrete. Let us compare the stress relaxation losses in the traditional steel reinforcement and the composite reinforcement. All data has been taken from the official regulations [14]. The full values of the first and second losses in the steel reinforcement were considered. Fig. 7 presents the theoretical extrapolation of the relaxation curves in glass and carbon compared with [14] for steel reinforcement at the same stress level.

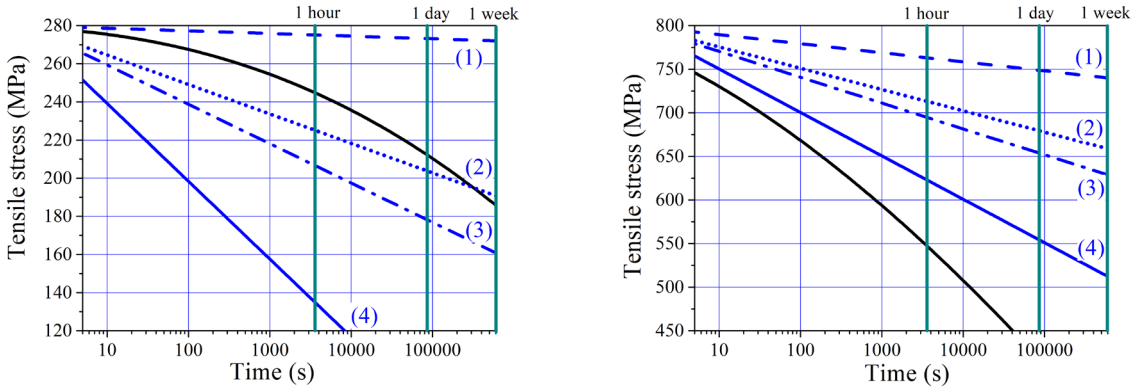

Figure 7. Theoretical extrapolation of the relaxation curves in glass (a) and carbon (b) compared with [12] for steel reinforcement at the same stress level.

The relationships obtained show that different types of losses have varying effects on the decay of internal stresses in the steel reinforcement. The minimum losses are observed when applying the formula for the mechanical losses due to the stress relaxation in the reinforcement (Curve 1). These amounts to no more than a few percent of the initial stress level. A similar trend was noted for carbon sheets in [11], where the reduction was approximately from 2 % to 4 % of the pre-stress level. If, in addition to the relaxation losses, other types of losses are considered (for example, from the temperature difference in the concrete heating), the stress loss becomes more significant (Curve 2). The total value of the immediate losses (from deformation, mechanical relaxation, temperature effects, and deformation of the steel form during non-simultaneous tensioning of the reinforcement) is described by Curve 3. If the time-dependent losses (namely, losses from anchor deformation and concrete shrinkage) are additionally considered and summed with the immediate losses, Curve 4 is obtained, which corresponds to the values of the total immediate and time-dependent losses in the steel reinforcement. Reference [11] also notes that the largest contribution to mechanical losses comes from losses due to insufficient anchorage, amounting to approximately from 12 % to 18 % of the prestress level.

Comparing the losses in the traditional steel reinforcement with the composite reinforcement, the stress relaxation curves for a comparable strain level were additionally plotted on the graphs. An analysis of these curves shows that the results obtained for the composites are close to the range of mechanical losses for the steel reinforcement. It should be considered that not all loss types of steel are inherent to the prestressing process of composites. Therefore, as in the case of glass roving, the total values of the immediate and time-dependent losses may not differ significantly from the stress relaxation curve for GFRP. In the case of glass roving, it is evident that the losses due to stress relaxation are quite large and even exceed the total immediate and time-dependent losses for traditional steel reinforcement. However, as the experiment showed, problems arise with the anchorage of the reinforcement, since pull-out tests demonstrate that a more flattened reinforcement cross-sectional shape improves the mechanical properties of the concrete composites. Hence, it can be concluded that the primary losses in the obtained data are attributable to the clamping device. This conclusion agrees with the findings in reference [11].

Losses due to mechanical relaxation for composite materials are essentially negligible, as glass and carbon rovings are not prone to stress relaxation in the same way as steel. Only a slight relaxation (a few percent) may occur within these rovings due to the interfiber friction in the roving. Accordingly, all major losses are attributed to the clamping device. Unfortunately, in the manufacturing of pre-stressed concrete composites with fibrous reinforcement, this is a primary issue, as the fibers are quite brittle and require the development of special anchoring devices. Such work is already underway, and the authors of this paper have proposed some fundamentally new solutions [15].

4. Conclusions

This study involved testing two types of rovings: glass and carbon, used as composite reinforcement for prestressed concrete structures. Testing was conducted at four levels of pre-stress – from 10 % to 40 % of the ultimate tensile load, in 10 % steps. Both direct and inverse stress relaxation was investigated.

A phenomenological description of the stress relaxation and inverse relaxation curves in glass and carbon rovings is proposed. Two parameters were required to describe the stress relaxation curves; a third was required to describe the inverse relaxation. Within the proposed description, the process of increasing

load and the process of decreasing load are described by different formulas. The results of the mathematical modeling showed satisfactory agreement with the experimental data.

As a practical application, the case of mechanical losses in traditional steel reinforcement was considered, for which curves were plotted according to the relevant regulation for steel reinforcement. A comparison of the stress relaxation results for the investigated materials with the data for the steel reinforcement was carried out. Recommendations are given for the practical application of the obtained data on the stress relaxation of fibrous composite reinforcement in pre-stressed concrete structures.

References

1. Choo, B.S. Reinforced and prestressed concrete. Advanced Concrete Technology. 4: Testing and Quality. Butterworth-Heinemann. Oxford, 2003. Pp. 3–17.
2. El-Hacha, R., Wight, R.G., Green, M.F. Prestressed Carbon Fiber Reinforced Polymer Sheets for Strengthening Concrete Beams at Room and Low Temperatures. Journal of Composites for Construction. 2004. 8(1). Pp. 3–13. DOI: 10.1061/(ASCE)1090-0268(2004)8:1(3)
3. Wang, H.T., Liu, S.S., Zhu, C.Y., Xiong, H., Xu, G.W. Experimental Study on the Flexural Behavior of Large-Scale Reinforced Concrete Beams Strengthened with Prestressed CFRP Plates. Journal of Composites for Construction. 2022. 26(6). Article no. 04022076. DOI: 10.1061/(ASCE)CC.1943-5614.0001246
4. Wang, H.T., Wu, G. Bond-slip models for CFRP plates externally bonded to steel substrates. Composite Structures. 2018. 184. Pp. 1204–1214. DOI: 10.1016/j.compstruct.2017.10.033
5. Lees, J.M., Winistoerfer, A.U. and Meier, U. External Prestressed Carbon Fiber-Reinforced Polymer Straps for Shear Enhancement of Concrete. Journal of Composites for Construction. 2002. 6(4). Pp. 249–257. DOI: 10.1061/(ASCE)1090-0268(2002)6:4(249)
6. Wight, R.G., Green, M.F., Erki, M.A. Prestressed FRP Sheets for Poststrengthening Reinforced Concrete Beams. Journal of Composites for Construction. 2001. 5(4). Pp. 214–220. DOI: 10.1061/(ASCE)1090-0268(2001)5:4(214)
7. Zdanowicz, K., Kotynia, R., Marx, S. Prestressing concrete members with fiber-reinforced polymer reinforcement: State of research. Structural Concrete. 2019. 20. Pp. 872–885. DOI: 10.1002/suco.201800347
8. Kim, Y.J., Green, M.F., Wight, R.G. Prestressed fiber-reinforced polymer (FRP) composites for concrete structures in flexure: fundamentals to applications. Advanced Composites in Bridge Construction and Repair. Woodhead Publishing. Cambridge, 2014. Pp. 30–60. DOI: 10.1533/9780857097019.1.30
9. Peled, A. Pre-tensioning of fabrics in cement-based composites. Cement and Concrete Research. 2007. 37(5). Pp. 805–813. DOI: 10.1016/j.cemconres.2007.02.010
10. Cao, Q., Zhou, J.P., Wu, Z.M., Ma, Z.J. Flexural behavior of prestressed CFRP reinforced concrete beams by two different tensioning methods. Engineering Structures. 2019. 189. Pp. 411–422. DOI: 10.1016/j.engstruct.2019.03.051
11. Haas, R., Quadflieg, T., Stolyarov, O. Analysis of reinforcement efficiency and microscopic characterization of glass and carbon roving geometry in prestressed concrete composites. Journal of Composite Materials. 2021. 55(23). Pp. 3293–3305. DOI: 10.1177/00219983211013382
12. Lou, T., Lopes, S., & Lopes, A. Time-dependent behavior of concrete beams prestressed with bonded AFRP tendons. Composites Part B: Engineering. 2016. 97. Pp. 1–8. DOI: 10.1016/j.compositesb.2016.04.070
13. Du, Y., Zhang, X., Liu, L., Zhou, F., Zhu, D., Pan, W. Flexural Behaviour of Carbon Textile-Reinforced Concrete with Prestress and Steel Fibres. Polymers. 2018. 10(1). Article no. 98. DOI: 10.3390/polym10010098
14. Li, J., Wang, M., Yue, Q., Liu, X. Transverse compressive properties, long-term stress relaxation, and post-relaxation properties of unidirectional CFRP composites. Journal of Building Engineering. 2025. 105. Article no. 112526. DOI: 10.1016/j.jobe.2025.112526
15. Wang, W.W., Dai, J.G., Harries, K.A., Bao, Q.-H. Prestress Losses and Flexural Behavior of Reinforced Concrete Beams Strengthened with Posttensioned CFRP Sheets. Journal of Composites for Construction. 2012. 16(2). Pp. 207–216. DOI: 10.1061/(ASCE)CC.1943-5614.0000255
16. Ornaghi, H.L., Almeida, J.H.S., Monticeli, F.M., Neves, R.M. Stress relaxation, creep, and recovery of carbon fiber non-crimp fabric composites. Composites Part C: Open Access. 2020. 3. Article no. 100051. DOI: 10.1016/j.jcomc.2020.100051
17. Umarov, B.S., Zinnurov, T.A. Studying stress losses in fiberglass reinforcement during relaxation and creep. Vestnik MGSU. 2025. 20(1). Pp. 50–59. DOI: 10.22227/1997-0935.2025.1.50-59
18. Pisani, M.A. Long-term behaviour of beams prestressed with aramid fibre cables: Part 1: a general method. Engineering Structures. 2000. 22(12). Pp. 1641–1650. DOI: 10.1016/S0141-0296(99)00107-8
19. Pisani, M.A. Long-term behaviour of beams prestressed with aramid fibre cables: Part 2: an approximate solution. Engineering Structures. 2000. 22(12). Pp. 1651–1660. DOI: 10.1016/S0141-0296(99)00108-X
20. SP 63.13330.2018. Concrete and reinforced concrete structures. General provisions. Ministry of Construction, Housing and Utilities of the Russian Federation. Moscow, 2019. 119 p.
21. Wang, H.T., Wu, Q., Zhu, C.Y., Mao, Y.H., Guo, C.C. An innovative prestressing system of prestressed carbon fiber sheets for strengthening RC beams under flexure. Construction and Building Materials. 2024. 411. Article no. 134409. DOI: 10.1016/j.conbuildmat.2023.134409
22. Piatek, B., Siwowski, T., Michalowski, J., Blazewicz, S. Flexural Strengthening of RC Beams with Prestressed CFRP Strips: Development of Novel Anchor and Tensioning System. Journal of Composites for Construction. 2020. 24(3). Article no. 04020015. DOI: 10.1061/(ASCE)CC.1943-5614.0001020
23. Yang, J., Johansson, M., Al-Emrani, M., Haghani, R. Innovative flexural strengthening of RC beams using self-anchored prestressed CFRP plates: Experimental and numerical investigations. Engineering Structures. 2021. 243. Article no. 112687. DOI: 10.1016/j.engstruct.2021.112687
24. Stolyarov, O., Quadflieg, T., Gries, T. Effects of fabric structures on the tensile properties of warp-knitted fabrics used as concrete reinforcements. Textile Research Journal. 2015. 85(18). Pp. 1934–1945. DOI: 10.1177/0040517515578334

25. Zhang, J. Modeling of the influence of fibers on creep of fiber reinforced cementitious composite. Composites Science and Technology. 2003. 63(13). Pp. 1877–1884. DOI: 10.1016/S0266-3538(03)00160-X
26. Ghasemi, R., Safarabadi, M., Haghighi-Yazdi, M., Mirdehghan, S.A. Experimental and analytical study of flexural creep of impregnated woven fabric-reinforced concrete. Composite Structures. 2023. 321. Article no. 117192. DOI: 10.1016/j.compstruct.2023.117192

Information about the authors:

Pavel Mostovykh, *PhD in Physics and Mathematics*

ORCID: https://orcid.org/0000-0003-3714-2996

E-mail: mostovykh_ps@spbstu.ru

Anna Dontsova,

ORCID: https://orcid.org/0000-0002-9081-9575

E-mail: anne.dontsoova@gmail.com

Tatiana Koriakovtseva, *PhD in Technical Sciences*

ORCID: https://orcid.org/0000-0002-8380-0067

E-mail: tamusorina@mail.ru

Oleg Stolyarov, *PhD in Technical Sciences*

ORCID: https://orcid.org/0000-0002-2930-5022

E-mail: stolyarov_on@spbstu.ru

Received 13.09.2025. Approved after reviewing 07.11.2025. Accepted 07.11.2025.